22nd International Conference on Renewable Energies and Power Quality (ICREPQ'24)

Bilbao (Spain), 26th to 28th June 2024

ISBN: 978-84-09-60656-6

Measurement methods to assess conducted emissions in the 9-150 kHz range generated by photovoltaic installations

U. Txertudi[1], G. Txertudi[1], A. Gallarreta[1], M. Fernández[1], I. Fernández[1], and D. de la Vega[1]

[1] University of the Basque Country (UPV/EHU)
48013 Bilbao (Spain)
Phone number: +34 946014133

Abstract. The increasing integration of inverter-based devices in the distribution grid is generating higher levels of conducted emissions in the 9-150 kHz range. The lack of standard measurement methods in this band has led to the development of new methods, which still require further evaluation. In this study, several measurement methods are analysed in the assessment of conducted emissions generated by a photovoltaic (PV) installation in the 9-150 kHz range. The paper describes the methods selected for the comparison and the measurement campaign specifically developed in this study to obtain recordings of emissions from different configurations of the PV panels. The results show that some of the novel methods provide accurate results and require lower computational burden and memory resources than the standard methods.

Key words. Conducted Emissions, Measurement Methods, Electromagnetic Interference, Power Quality, Photovoltaic Energy.

1. Introduction

The increasing integration of electronic devices in the low-voltage (LV) distribution power grid has led to the presence of non-intentional emissions (NIE) in the form of conducted emissions in frequencies up to 150 kHz. The NIE in the 9-150 kHz range are primarily generated by inverter- and rectifier-based devices, such as photovoltaic (PV) panels, battery chargers, hydropower systems, and wind turbines [1]-[3]. In photovoltaic inverters, the emissions are often in the form of multiples of the switching frequency of the inverter, in some cases covering the whole range up to 150 kHz [1].

The conducted NIE have the potential of degrading the Power Quality (PQ) and affecting the Power Line Communications (PLC) between devices connected to the grid [4]. Furthermore, they can potentially damage the equipment connecting to the grid, causing aging, thermal stress or malfunctioning [2],[5]. For these reason, the characterization of these disturbances becomes necessary to evaluate all these effects.

The regulatory framework to measure conducted disturbances are well-defined for frequencies up to 2 kHz and between 2 kHz and 9 kHz [6]. However, the 9-150 kHz band lacks of normative standardized measurement methods: although Annex C of the IEC 61000-4-30 Ed. 3 standard proposes three measurement approaches, they have non-normative consideration and the description of the approaches shows some unsolved aspects for the use of these non-normative methods in the 9-150 kHz range [7].

In light of these challenges, recent research endeavours have proposed novel measurement methods aimed at achieving accurate and consistent assessments of NIE in the 9-150 kHz band, some of them focused on demanding a lower computational burden and reduced assessment resources and memory requirements. Although these novel methods may be useful in some specific measurement cases, their performance needs still to be evaluated in different scenarios (specific sources of NIE and grid topologies).

This study aims at evaluating the performance of measurement methods in the assessment of conducted NIE generated from PV panels in the 9-150 kHz range. For this purpose, a set of methods is selected and applied in a measurement campaign in a PV installation. The performance of the measurement methods is analysed by comparing the results of all the methods through a statistical analysis of the measurement results.

2. Measurement methods for conducted emissions in the electrical grid

A. Criteria for the selection of the measurement methods

The metrics to evaluate different aspects of the conducted emissions are the first selection criterion. The selected methods should include root mean square (RMS) and quasi-peak (QP) detectors: the RMS detector provides information about the energy of the disturbances and the QP detector is needed for the comparison with Compatibility Levels (CL) in the 9-150 kHz range, as the CL are defined in QP values in this range by the IEC 61000-2-2 [8].

The second criterion is the use of standard methods, or methods with an approach close to the standard methods, as they try to complete or emulate their performance or the type of results.

Hence, for obtaining RMS measurement results, two methods are selected. Firstly, the method described in Annex B of IEC 61000-4-7 standard, which is defined for frequencies up to 9 kHz [6], is directly applied in this analysis to the 9-150 kHz frequency range. Secondly, a recently published adaptation of the IEC 61000-4-7 to frequencies above 9 kHz, also providing higher time granularity and better frequency allocation of emissions is selected for the study. This method is referred as RM-A method [9].

For the QP assessment, the CISPR16-1-1 receiver [10] and two recently published methods focused on reducing some of the drawbacks of the CISPR 16-1-1 receiver (the Light-QP [11] and the Statistical-QP methods [12]) are selected.

B. Description of the selected measurement methods for the assessment of RMS values

1) Extension of the IEC 61000-4-7 method to the 9-150 kHz range

The IEC 61000-4-7-Annex B method is defined for the 2-9 kHz frequency band [6]. The IEC 61000-4-30 suggests extending this technique for the 9-150 kHz frequency band, although it does not specify how to adapt it to a considerably wider frequency range [7], which implies a greater computational burden. As it is shown in Fig. 1, this method is composed of two stages: spectral analysis and frequency grouping. Firstly, rectangular non-overlapped 200 ms windows are applied to compute the short-time Fourier transform (STFT), which results in frequency components with a 5 Hz resolution bandwidth. These components are then integrated to form 200 Hz bandwidth components (see equation (1))

$$Y_{B,b} = \sqrt{\sum_{f=b-95Hz}^{b+100Hz} Y_{C,f}^{\ 2}} \qquad (1)$$

Where b is the corresponding center frequency, from 2.1 to 8.9 kHz. This grouping is asymmetric, since the number of components above and below the central frequency is different. Finally, the RMS values for 200 Hz frequency bins are calculated every 3 seconds, in accordance with IEC 61000-4-30 [12].

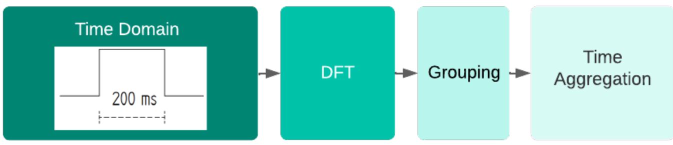

Fig. 1. Main steps of the IEC 61000-4-7 method

2) RM-A method

Based on the Annex B of IEC 61000-4-7:2002+AMD 1:2008, the RM-A method adapts the implementation of this method to the frequency range 9-150 kHz (CISPR Band A) [9]. The method provides spectra of RMS and maximum values with 200 Hz bandwidth and 20 ms time resolution.

With respect to IEC 61000-4-7, the RM-A method changes the window size of the STFT from 200 ms to 20 ms, while maintaining non-overlapped rectangular windows. This ten times shorter time windowing improves the time granularity of the results.
In the frequency domain, 50 Hz bandwidth samples are obtained; then, a symmetrical frequency grouping is proposed in this method to obtained 200 Hz bandwidth outputs, as it is shown in Fig. 2 and equation (2).

$$Y_{B,b} = \sqrt{\frac{1}{2} Y_{C,b-100Hz}^{\ 2} + \sum_{f=b-50Hz}^{b+50Hz} Y_{C,f}^{\ 2} + \frac{1}{2} Y_{C,b+100Hz}^{\ 2}} \quad (2)$$

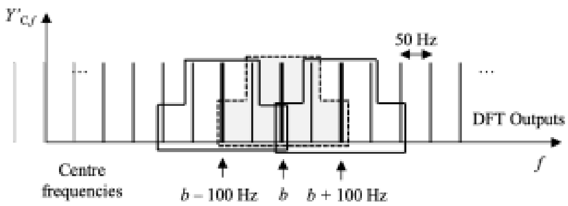

Fig. 2. Symmetrical grouping of frequency components in RM-A measurement method [9].

C. Description of the selected measurement methods for the assessment of QP outputs

1) CISPR16-1-1 receiver

The CISPR16-1-1 method defines a QP-type detector that allows the comparisons with CL in the CISPR Band A [10]. The method is defined by a black-box receiver approach that must fulfill a set of performance conditions. Some of these specifications correspond to the response of analog components in the front-end, and the standard does not define a digital implementation, even though they are allowed. The performance of the receiver is defined by the response to a set of test signals in the form of periodical pulses.

The method applies 20 ms Lanczos time windowing with a high level of overlap. The outputs of the time windowing are used in the STFT to obtain frequency components with a frequency step size of 50 Hz. Then, a QP detector based on the performance of an analog RC circuit and a critically damped meter is defined in the standard (see Fig. 3) [11].

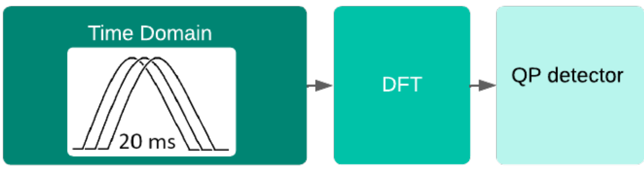

Fig. 3. Main steps of the CISPR-16 method

As the definition of the CISPR 16-1-1 receiver allows large tolerances in its implementation, a wide number of compliant implementations is allowed. Nevertheless, the digital implementation is not defined in the standard. In this study, the digital CISPR 16-1-1 receiver published in [11] is used in the analysis.

2) Light-QP method

The Light-QP method uses the RM-A method as the first stage of the overall method. Hence, the RM-A method obtains RMS values, which are used as input values for the following stage of the method. The second stage of the method involves the implementation of a digital QP detector based on the use of digital filters, which replicate both the analog behavior of the RC circuit and the critically damped meter as defined by the standard [11].

The computational burden of the Light-QP method, measured by the number of fast Fourier transforms, is 10 times lower with respect to the CISPR 16-1-1 method. Additionally, the memory requirements are over 100 times lower for computing the spectrogram and more than 10 times lower for obtaining quasi-peak outputs [11].

3) Statistical QP method

The Statistical-QP method also applies the RM-A method in the first stage of the overall method, in order to obtain RMS values. The second stage calculates QP values based on the results of a previous statistical analysis that relates RMS and QP values [12]. Hence, this method applies a conversion factor to obtain equivalent QP values from the RMS values provided by the RM-A method. Some studies have demonstrated that the amplitude values obtained by the Statistical QP method are similar to the CISPR 16 QP spectra in some scenarios [12]. Nevertheless, further analysis should be developed in different scenarios with other sources of conducted emissions.

3. Methodology

A set of conducted emissions were recorded in a measurement campaign at the photovoltaic laboratory at UPV/EHU. In the trials, several configurations of PV panels were measured, including series and parallel setups, as well as grid-connected or isolated. Then, the methods under study were applied to the raw recordings of the conducted emissions for comparison, in order to evaluate the performance of the methods for emissions from PV panels in different configurations.

A. Acquisition system and measurement campaign

The signals used to compare the outputs of measurement methods under study were recorded using an acquisition system developed by the UPV/EHU [4],[14]. The acquisition system for the measurement of conducted emissions is composed of a voltage probe, a digital oscilloscope, and a laptop. The voltage probe implements a bandpass filter for the 9-500 kHz range and galvanic isolation in order to get rid of the conducted emissions outside the band of interest and to protect the equipment from overvoltages, respectively. The oscilloscope digitizes the filtered signal with a resolution of of 16-bits and a sampling frequency of 8.92 MS/s. Finally, the laptop controls the oscilloscope, in order to set the measurement parameters and store the raw data.

Measurements were carried out at four different PV installations located inside a laboratory, while solar panels were placed in an outdoor terrace next to the laboratory. Specifically, conducted emissions from two standalone and two grid-connected systems were recorded. The standalone installations employ a Maximum Power Point Tracking (MPPT) load regulator, a 12 V battery, and the TBS PS600-12 inverter model. They also have the necessary magnetothermal and differential switches to ensure safety. Both systems employ two 80-watt peak (Wp) monocrystalline panels. The difference between both lies in the panel connections: in one, the panels are connected in series, and in the other one, in parallel.
Regarding the grid-connected installations, the first system employs two monocrystalline panels connected in series, which can provide a total maximum power of 350 Wp, and the Mastervolt SOLADIN 600 inverter. The other grid-connected system can provide 1110 Wp due to its six panels connected in series and uses the Fronius IG 15 inverter. Both installations have magnetothermal and corresponding differential switches.

B. Statistical analysis of the results

The comparison of the performance of the methods is developed by applying a statistical analysis to the results provided when they are applied to the recordings of the measurement campaign. The statistical analysis is applied separately for RMS and QP outputs; therefore, the comparison is developed separately for RMS methods (IEC 61000-4-47 and RM-A) and QP methods (CISPR 16-1-1, Light-QP and Statistical-QP).

The statistical analysis evaluates the differences (in absolute values), in terms of the median value and the standard deviation, and the relative differences, in terms of the median value and the comparison against the 2% and 10% of the corresponding CL at that frequency (as the CL vary with frequency along the 9-150 kHz range). This last aspect allows the evaluation of the results with respect to a known and standardized reference level.

Moreover, in the analysis, the effects of the calculation procedures on the final outputs is also evaluated, as these aspects may determine the time and frequency resolution, or have an impact on the accuracy of the results.

4. Results and Analysis

This section contains the results for the comparison between the methods under study and the analysis of the deviations in the spectral outputs.

A. Results in the assessment of RMS outputs

The results of the statistical analysis of the methods providing RMS outputs are summarized in Table I and Fig. 4. The comparison of the outputs of RMS values from IEC 61000-4-7 and RM-A methods shows that the absolute differences in magnitude are always within a few

TABLE I

COMPARISON OF DEVIATION FOR METHODS PROVIDING RMS OUTPUTS

Comparison	Absolute value of differences			Relative differences		
	Median	95^{th}	Range of 80 % (90^{th} -10^{th})	Median	Perc. of diff. ≤5 % of CL	Perc. of diff. ≤10 % of CL
IEC 61000-4-7 vs. RM-A	-0.018 mV	2.404 mV	1.811 mV	3.21 %	98.92 %	99.82 %

TABLE II

COMPARISON OF DEVIATION FOR METHODS PROVIDING QP OUTPUTS

Comparison	Absolute value of differences			Relative differences		
	Median	95^{th}	Range of 80 % (90^{th} -10^{th})	Median	Perc. of diff. ≤5 % of CL	Perc. of diff. ≤10 % of CL
CISPR 16 vs. Light-QP	0.012 mV	1.795 mV	1.283 mV	3.84 %	99.91 %	99.99 %
CISPR 16 vs. Statistical-QP	0.087 mV	1.746 mV	1.487 mV	3.94%	99.86%	99.98%

millivolts in the entire 9-150 kHz range, with a median value close to 0 mV, the 95^{th} of differences below 2.40 mV and the dispersion for the 80% of the differences being of 1.8 mV. Moreover, the median relative difference is of 3.2% (see Table I). It is remarkable that the 98.92% of the frequency bands exhibit differences lower than 5% of the Compatibility Limits (CL), while 99.82% register variances below 10% of the CL.

Therefore, the results show that the RM-A method provides results similar to those obtained by the IEC 61000-4-7 method. Moreover, the RM-A method was designed to provide a greater time resolution and to reduce computational time and requirements, by modifying the window size of the STFT from 200 ms to 20 ms.

B. Methods based on the assessment of QP outputs

The comparison between the results provided by CISPR 16-1-1 receiver and Light-QP is shown in Table II and Fig. 5. The results for Light-QP method are consistent with those of the CISPR 16 approach: the median relative differences remain below 4%, with 99.91% of recorded variances below 5% of CL, and 99.99% indicating variances lower than 10% of CL. Regarding the absolute results, the median absolute deviation is close to 0 mV, the 95^{th} percentile of the differences below 1.8 mV and the range of the 80% of the samples within 1.3 mV (see Table II).

The evaluation between the results provided by CISPR 16-1-1 receiver and Statistical-QP is shown in Table II and Fig. 6. It can be observed that the absolute differences in magnitude fall within a few millivolts across the entire 9–150 kHz spectrum, with a median absolute difference of 0.08 mV, a dispersion for the 80% of the differences being within 1.5 mV and the 95^{th} percentile of the deviation been lower than 1.8 mV. In addition, the mean relative difference is below 4%, which is a typical uncertainty value for PQ instruments [6]. Notably, 99.86% of the frequency bands exhibit differences lower than 5% of the Compatibility Limits (CL), while 99.98%showcase variances below 10% of the CL (see Table II).

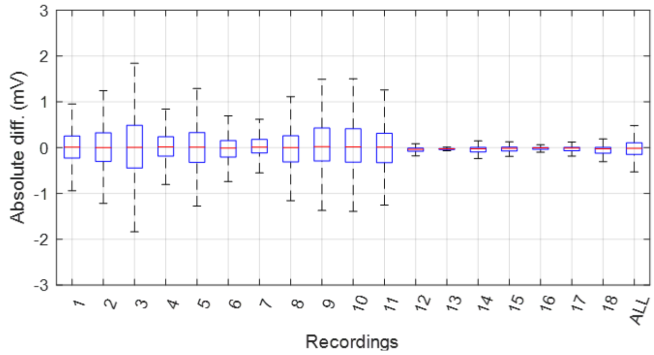

Fig. 4. Absolute values of the differences between the RMS spectra of IEC 61000-4-7 and RM-A

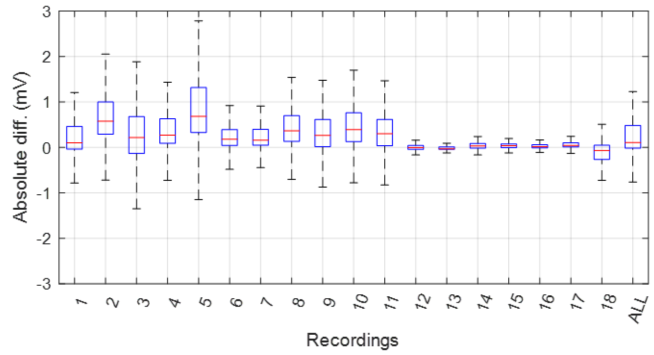

Fig. 5. Absolute values of the differences between the QP spectra of CISPR16 and Light QP

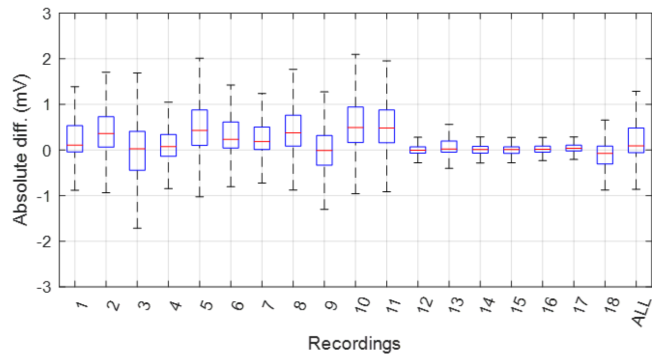

Fig. 6. Absolute values of the differences between the QP results of CISPR16 and Statistical QP.

Therefore, the results of the analysis show that the amplitude values obtained with the Statistical QP are similar to the CISPR 16-1-1 receiver. However, the computational load and memory demands for executing the Statistical-QP are substantially lower than the required for CISPR 16-1-1. The main reason is that the Statistical-QP does not include a Quasi-Peak detector. Therefore, this method requires less assessment resources, making it more cost-effective for simpler Power Quality instruments to be deployed in extensive monitoring campaigns.

From the observations, it can be concluded that both the Statistical-QP and Light QP methods provide similar results to a digital implementation of the CISPR16 receiver, as 90% of differences vary within a few millivolts for individual recordings and remaining below +/- 1 mV for the complete set of recordings.

The analysis of the CISPR 16 method leads to confronted conclusions. On one hand, the CISPR-16 is the method with the highest frequency and temporal resolution. Moreover, it provides lower background noise level due to the Lanczos windowing and better accuracy in peaks and emissions where the peak and the average are equal. On the other hand, the CISPR-16 method was designed for carrying tests under laboratory conditions, and the implementation of this method to measurements in the field is not direct. Additionally, it allows large tolerances in its implementation, leading to a wide range of valid results for a given input [13].

Regarding the Light QP and the Statistical-QP methods, they are suitable for field measurements of the electrical grid and they are not limited to controlled laboratory conditions. Furthermore, the complexity, the computational burden, and the memory requirements of this method are significantly lower than the required by CISPR 16, thus enabling simple instruments for field measurements.

5. Conclusions

The analysis developed in this study allows the evaluation of the performance of a set of measurement methods to assess the conducted emissions in the 9-150 kHz frequency range.

To obtain information about the energy of the emissions, two measurement methods that provide RMS values have been selected: the direct application of the IEC 61000-4-7 standard to the 9-150 kHz range, and the RM-A method, which incorporates some changes to adapt this standard and to obtain higher accuracy in both time and frequency domains.

The results in the assessment of emissions from PV panels show that both methods provide similar results in frequency, but in the time domain, the RM-A method provides a granularity 10 times more precise, due to the use of a shorter time window in the signal processing. This aspect provides a better identification of impulsive noise, as short impulses are not averaged in longer intervals, as it can occur in the IEC 61000-4-7 method.

The QP detector provides values that include information about the variability of the emissions over the time and, for this reason, it is the metric selected in the 9-150 kHz range to compare the magnitude of the conducted emissions to the CL. The methods selected in this evaluation are the CISPR 16-1-1 QP receiver, based on the response of a RC circuit and a critically damped meter, and two recently developed methods that provide QP outputs with lower computational and memory resources. These are the Light-QP method, based on a digital implementation of the QP detector defined in the CISPR 16-1-1 standard, and the Statistical-QP method, based on statistical results of the comparison of RMS and QP values.

The results of these methods, when they are applied to emission generated by PV panels, show that the magnitudes of the outputs of all the QP methods are similar, and none of the methods seems to lose relevant information of the grid disturbances. Moreover, the Statistical-QP method and the Light-QP method provide RMS values as an intermediate result, which is consistent with RMS values calculated below 9 kHz (this is, 200 Hz resolution bandwidth RMS values).

As the Statistical-QP method and the Light-QP method require less computational burden and, therefore, they could be implemented in simpler and cheaper receivers, they seem to be good candidates for its use in grid monitoring, where extensive measurement campaigns based on a high number of receivers are developed.

This contribution aims to consolidate and extend the accuracy analysis of the novel RM-A, Light-QP and Statistical-QP methods by evaluating their performance with recordings not used during the validation of the methods. Moreover, in the future, these methods should be implemented on low-cost devices, with reduced memory and processing resources, in order to evaluate the feasibility of being implemented on this type of platforms. The ultimate goal of this viability analysis is to be able to deploy these meters massively in the network and to monitor conducted emissions in the 9-150 kHz range.

References

[1] Fernandez, I.; Uribe-Pérez, N.; Eizmendi, I.; Angulo, I.; de la Vega, D.; Arrinda, A.; Arzuaga, T. Characterization of non-intentional emissions from distributed energy resources up to 500 kHz: A case study in Spain. Int. J. Electr. Power Energy Syst. 2019, 105, 549–563.

[2] V. Khokhlov, J. Meyer, P. Schegner, D. Agudelo-martinez, A. Pavas, “Immunity assessment of household appliances in the frequency range from 2 to 150 kHz”, 25th International Conference on Electricity Distribution (CIRED), Madrid, 2019, doi: 10.34890/283.

[3] L. Sandrolini, A. Mariscotti, “Waveform and Spectral Characteristics of Supraharmonic Unsymmetrical Conducted EMI of Switched-Mode Power Supplies”, Electronics, 2022, doi: 10.3390/electronics11040591.

[4] I. Fernández, D. de la Vega, A. Arrinda, I. Angulo, N. Uribe-Pérez, and A. Llano, “Field trials for the characterization of non-intentional emissions at low-voltage grid in the frequency range assigned to NB-PLC technologies” Electronics, Vol. 8, 2019, doi: 10.3390/electronics8091044.

[5] A. Espín-Delgado, S. Rönnberg, S. Sudha Letha, M. Bollen, "Diagnosis of supraharmonics-related problems based on the effects on electrical equipment",in Electric Power Systems Research,Vol. 195, 2021, doi: 10.1016/j.epsr.2021.107179.

[6] International Electrotechnical Commission, “Electromagnetic compatibility (EMC) - Part 4-7: Testing and measurement techniques - General guide on harmonics and interharmonics measurements and instrumentation, for power supply systems and equipment connected thereto”, doc. IEC 61000-4-7:2002+AMD1:2008.
[7] International Electrotechnical Commission, “Electromagnetic compatibility (EMC) - Part 4-30: Testing and measurement techniques - Power quality measurement methods”, doc. IEC 61000-4-30 Ed.3, 2015.
[8] Electromagnetic compatibility (EMC) - Environment - Compatibility levels for low-frequency conducted disturbances and signalling in public low-voltage power supply systems, IEC 61000-2-2:2002+A2:2019 Ed. 2.2, 2002.
[9] A. Gallarreta, I. Fernández, D. Ritzmann, S. Lodetti, V. Khokhlov, P. Wright, J. Meyer, D. de la Vega, “Adaptation of the IEC 61000-4-7 Measurement Method to CISPR Band A (9-150 kHz)”, 2022 IEEE 12th Int. Workshop on Applied Measurements for Power Systems, Cagliari, Italy, 2022, doi: 10.1109/AMPS55790.2022.9978818.
[10] International Electrotechnical Commission, “Specification for radio disturbance and immunity measuring apparatus and methods - Part 1-1: Radio disturbance and immunity measuring apparatus - Measuring apparatus”, CISPR 16-1-1:2019, 2019.
[11] A. Gallarreta, I. Fernández, D. Ritzmann, S. Lodetti, V. Khokhlov, P. Wright, J. Meyer, D. de la Vega, “A Light Measurement Method for 9-150 kHz Disturbances in Power Grids Comparable to CISPR Quasi-Peak”, IEEE Transactions on Instrumentation and Measurement, 2022, doi: 10.1109/TIM.2022.3195255.
[12] A. Gallarreta, I. Fernández, D. Ritzmann, S. Lodetti, V. Khokhlov, D. de la Vega, P. Wright, J. Meyer, "Statistical relationship between RMS and QP spectra of voltage measurements in the 9–150 kHz range", Electric Power Systems Research, Vol. 218, doi: 10.1016/j.epsr.2023.109213.
[13] S. Lodetti, A. Gallarreta, D. Ritzmann, V. Khokhlov, P. Wright, J. Meyer, I. Fernández, D. de la Vega, "On the suitability of the CISPR 16 method for measuring conducted emissions in the 2–150kHz range in low voltage grids", Electric Power Systems Research, Vol. 216, 2023, doi: 10.1016/j.epsr.2022.109011.
[14] I. Fernández, M. Alberro, J. Montalbán, A. Arrinda, I. Angulo, and D. de la Vega, “A new voltage probe with improved performance at the 10 kHz–500 kHz frequency range for field measurements in LV networks”, Measurement, Vol. 145, 2019, doi: 10.1016/j.measurement.2019.05.106.